Sorption Studies of Neutral Red Dye onto Poly(acrylamide-*co*-maleic acid)-Kaolinite/Montmorillonite Composites

H. M. Abdel-Aziz, A. A. El-Zahhar, T. Siyam

Nuclear Chemistry Department, Hot Laboratories Center, EAEA, Cairo, Egypt, P.C. 13759

Received 12 December 2009; accepted 11 June 2011
DOI 10.1002/app.35067
Published online 4 October 2011 in Wiley Online Library (wileyonlinelibrary.com).

ABSTRACT: In this study, a procedure for preparation of organic–inorganic composite was established. The procedure was based on gamma irradiation polymerization of polyacrylamide (PAAm) in presence of maleic acid (MA), clay minerals [kaolinite (K)], or [montmorillonite (M)] and methylenebisacrylamide (NMBA) as a crosslinker. The functionality of the produced adsorbents were assayed using FTIR spectroscopy, SEM, and XRD and were evaluated for sorption of neutral red (NR) dye from aqueous solutions via batch sorption experiments. Various factors influencing the sorption behavior (e.g., pH, sorbent dose, and dye concentration) were studied. The sorption data fitted well with Langmuir isotherm model. Batch kinetic experiments showed that the adsorption followed pseudo-second-order kinetic model with correlation coefficients greater than 0.999. © 2011 Wiley Periodicals, Inc. J Appl Polym Sci 124: 386–396, 2012

Key words: sorption; polymer; clay; composites; organic dye

INTRODUCTION

Polymer/clay composites have been regarded as promising materials for many applications because of their unique properties, such as catalysis,[1] adsorption, packaging[2] electronic or photonic devices,[3] and insulation.[4,5] These nanocomposites are known to display enhanced mechanical, thermal, and fire retardancy properties[6] in comparison with their corresponding virgin polymers.

Clay minerals, such as kaolinite,[7,8] montmorillonite,[9–11] attapulgite,[12] mica,[13] bentonite, and sercite,[14] have all been used for the preparation of polymer composites. The incorporation of these mineral powders can not only reduce production cost, but also improve the properties (such as swelling ability, gel strength, mechanical and thermal stability) of polymer and accelerate the generation of new materials for special applications.[15] The unit structure of montmorillonite is composed of an aluminum oxide (octahedral) layer between two silicon oxide (tetrahedral) layers.[16] In the interlayer space, there are exchangeable cations e.g., Na^+, Ca^{2+}, Mg^{2+} etc, which can exchange with inorganic metal ions,[17] organic cationic surfactant, and cationic dyes.[18] Kaolinite, a 1 : 1 type clay mineral, is unique because the interlayer is sandwiched by hydroxyl groups on one side and oxide layers on the other side which may induce specific guest orientations.[19,20] The size and aspect ratio of kaolinite are larger than those of montmorillonite. Consequently, the interactions at the interfaces between kaolinite and polymers should be very different from those of smectite-polymer systems.

Montmorillonite is constructed of a single octahedral sheet sandwiched between two tetrahedral sheets.[21] Their crystal structure consists of two dimensional layers (thickness = 0.95 nm) formed by fusing two tetrahedral silica sheets with an edge-shared octahedral sheet of either alumina or magnesia.[22] Stacking of these layers leads to Van der Waals gaps or galleries. The galleries (alternatively referred to as interlayer) are occupied by cations, typically Na^+ and/or Ca^{2+}, which balance the charge deficiency that is generated by isomorphous substitution within the layers. The charge deficiency within the clay mineral layers is related to the following:[23]

1. Trivalent metal ions of the octahedral sheet may be replaced by bivalent ones (dioctahedral minerals, e.g., montmorillonite: $Al^{3+} \rightarrow Mg^{2+}$).
2. Bivalent metal ions of the octahedral sheet may be replaced by univalent one (trioctrahedral minerals).
3. Not all octahedral lattice sites (2/3 for the dioctrahedral and 3/3 for the trioctrahedral case) need to be occupied.
4. Si^{4+} ions in the tetrahedral sheet might have been substituted by Al^{3+}.

Correspondence to: H. M. Abdel-Aziz (hmabdelaziz@hotmail.com).

TABLE I
Chemical Formula and CEC of Clays Incorporated into the Polymeric Network

	Kaolinite	Na^+-montmorillonite
Chemical formula	$Al_4[Si_4O_{10}](OH)_8$	$(1/2Ca, Na)_{0.7}$ $(Al, Mg, Fe)_4$ $(Si, Al)_8O_{20}(OH)_4$
CEC (mmol/g)	3–15	70–130
Layer structure	1 : 1	2 : 1
Family of clay	Family of kaolinite	Family of saponitea
$n SiO_2/n Al_2O_3$	2 : 1	4 : 1

All the above results increase the negative charge within clay minerals. This negative charge is balanced by cations, the so called exchangeable cations. These cations are not structural and can be easily replaced by other positively charged ions or molecules in solutions.[24,25] The properties of clay minerals are closely associated with the crystal structure and it is essential to know the surface properties. A comparison of the characteristics of two common layered silicates of clay minerals is given in detail in Table I and Figure 1.

Pollution caused by textile wastewater is a common problem faced by many countries. Dyeing of wastewater in textile industry is generally high in both color and organic content. Some dyes are stable to biological degradation and may be toxic.[26] Some dyes are carcinogenic and mutagenic. The removal of color from textile wastewaters is a major environmental problem. Adsorption has evolved as one of the most effective processes for decoloration of textile wastewater.[27] Various polymeric clay composite have been used for the removal of acidic and basic dyes from aqueous solutions.[28–31]

In this work, P(AAm-MA)-K and P(AAm-MA)-M were prepared by gamma irradiation polymerization of polyacrylamide (PAAm) in presence of maleic acid (MA) and kaolinite or Na^+-montmorillonite micropowder using *N*,*N*-methylenebisacrylamide (NMBA) as a crosslinker. The sorption property of these polymer/clay composites for organic dye (NR) was studied from aqueous solutions. The influence of some experimental factors (pH, contact time, sorbent dosage, dye concentration, and sorption kinetics as well) were evaluated and discussed. The equilibrium data have been analyzed using various adsorption isotherms.

EXPERIMENTAL

Materials

All chemicals used in this study were of analytical grade reagent and were used without further purification. PAAm average molecular weight over 5,00,0000 and MA were obtained from Merck and Aldrich Chemicals, respectively. *N*,*N*′-methylenebisacrylamide (NMBA) was purchased from Merck, Kaolinite was supplied by Sigma, and Na^+-montmorillonite was purchased from Aldrich. They were used without further purification.

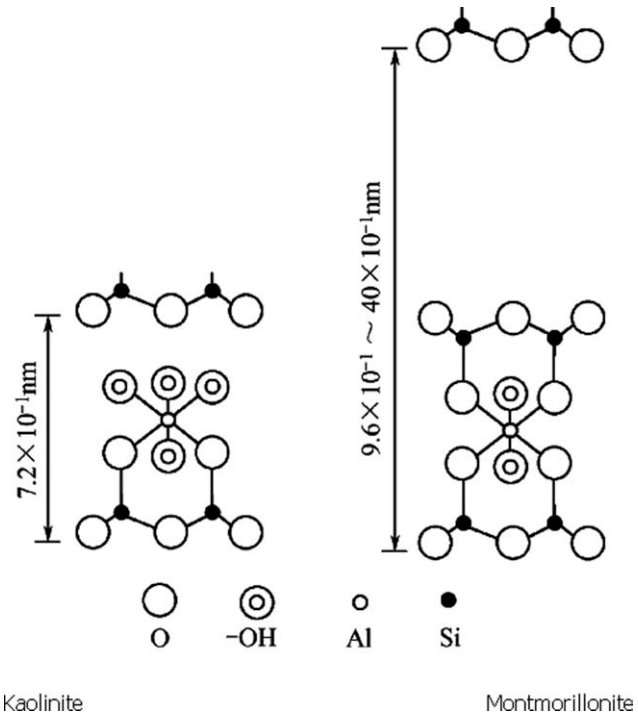

Figure 1 Characteristics of structure of kaolinite and montmorillonite.

Neutral red was obtained from Allied Chemical, whose structure is shown in Figure 2 below and was used as a neutral dye. Hydrochloric acid and sodium hydroxide solutions were used to adjust the pH of the aqueous solution.

Preparation of polymer/clay composites

Polymer/clay composites containing different kinds and amounts of clay were prepared according to the following procedure: 1 g NMBA and 3 g PAAm (in 50.0 mL distilled water) were introduced into a 250-mL-flask, equipped with stirrer, thermometer, and

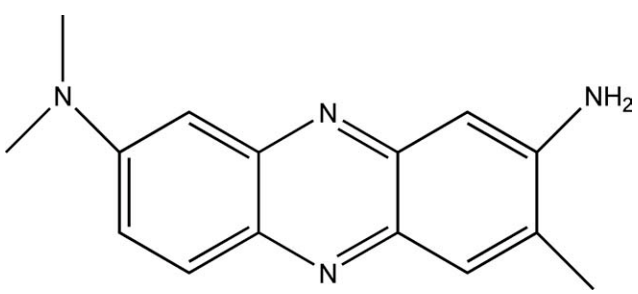

Figure 2 Structure of neutral red dye.

nitrogen gas aeration. The mixture was vigorously stirred till complete dissolution of NMBA, and then appropriate amount of clay (kaolinite or montmorillonite) was dispersed in the mixture. After being purged with nitrogen gas for 30 min (for removal of dissolved oxygen), the mixture was stirred for 2 h, and then 10 g of MA was introduced into the flask. The solution was stirred vigorously till obtaining complete homogeneity. Finally, the mixture was irradiated at ambient temperature in gamma radiation cell (MC-20 Russian) with dose of 30 kGy at fixed dose rate of 3.5 kGy h^{-1}. After irradiation, the composites were washed in acetone for removal of unreacted monomers, cut into small pieces, dried, ground, and stored for further use. The percent conversion was determined gravimetrically and was found to be 90%.

FTIR analysis

Infrared spectra of the prepared adsorbent samples (before and after dye adsorption) were obtained using FT-IR spectrometer with KBr disc (Bomen, Hartman and Borunz spectrometer, Model MB 157, Canada).

X-ray diffractometer

The X-ray diffraction patterns of the prepared polymer/clay composites were assayed using Shimadzu XD-DI X-ray diffractometer with scattering angle from 4° to 70° and scanning rate of 3°/min. Experiments were carried out at room temperature, and the basal spacing "*d*" was calculated using Bragg's equation.

Morphology of composites

The morphology of the prepared composites was determined using scanning electron microscope (SEM; Jeol JSM 60) at accelerating voltage of 15 kV.

Sorption Studies

Batch sorption experiments were carried out at 25°C ± 1°C in thermostatic water bath shaker (BS-21 JEIO TECH, Korea) at 180 rpm. In a glass 10 mg of P(AAm-MA)-K or P(AAm-MA)-M (surface area: 15.8, 15 m^2 g^{-1} and bead size: 60–80 mesh, respectively) was shacked within 20 mL of dye solution (concentration (200 mg L^{-1}). The dye concentrations in solution before and after experiments were determined spectrophotometrically at 530 nm. The amount adsorbed of dye was studied from aqueous solutions of pH from 1 to 7. The removal efficiency (*R*, %) and the adsorbed amount, *q* (mg/g) were calculated using the following expressions:

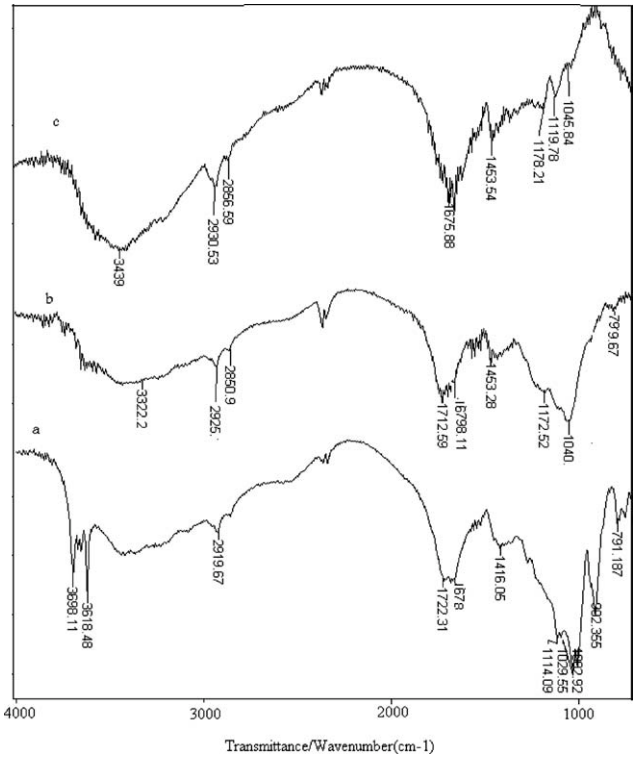

Figure 3 Infrared spectra of P(AAm-MA)-K (a), P(AAm-MA)-M (b), and P(AAm-MA) (c).

$$q(\mathrm{mg/g}) = \frac{(C_i - C_e)V}{m} \quad (1)$$

$$R = \frac{(C_i - Ce)}{C_i}100 \quad (2)$$

where C_i and C_e are the initial and equilibrium concentrations of dye (mg L^{-1}), respectively, V is the solution volume (l), and m is the adsorbent amount (g).

RESULTS AND DISCUSSION

FTIR spectra

The IR spectra of the prepared polymer/clay composites (before and after dye adsorption) are given in Figures 3 and 4. For P(AAm-MA)-K [Fig. 3(a)], the peak observed at 3698 cm^{-1}, corresponding to the *N*-H stretching of acrylamide unit. While the peaks observed at 2919 and 1722 cm^{-1}, could be assayed for —C—H stretching and the υ C=O of maleic acid, respectively. The peak at 1678 cm^{-1} could be due to the carbonyl moiety of the acrylamide unit, while the peak at 1420 cm^{-1} could be because of the olefinic C=C stretching vibration. Also the peak at 1029 cm^{-1}, corresponding to the Si—O stretching of kaolinite was observed.

The IR spectrum of P(AAm-MA)-M [Fig. 3(b)] showed different peaks. The peak observed at 3439

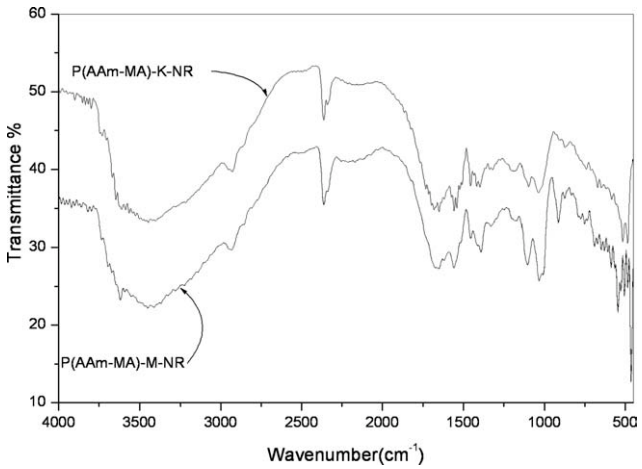

Figure 4 Infrared spectra of P(AAm-MA)-K-NR and P(AAm-MA)-M-NR.

cm^{-1} was assigned for the N—H stretching of acrylamide unit, while that observed at 2930 cm^{-1} could be attributed to the —C=H stretching vibration. The peak observed at 1712 cm^{-1} could be due to the υ C=O of maleic acid, while that observed at 1679 cm^{-1} was assigned for carbonyl moiety of the acrylamide unit. The peak observed at 1453 cm^{-1} was attributed to the carboxylic OH of maleic acid. Also there are absorption bands characteristic for Si—O—Al and Si—O were observed at 799 and 1040 cm^{-1}, respectively,.[32] The slight shift in the peaks positions in the IR spectrum may be because of the intercalation of montmorillonite and polymeric chains, which could be confirmed by XRD analysis and it agrees with previous work.[11] The intercalation of polymeric chains into montmorillonite could be caused by the weak Van der Waals forces between the hydrated exchangeable cations and oxygen atoms of carbonyl groups. Also hydrogen bonding may take part between the amide and carboxylic groups of PAAm and MA, respectively, with the oxygen atoms in the silicate sheets of montmorillonite.

Adsorbent dye interaction

The interaction between dye and (P(AAm-MA)-K or P(AAm-MA)-M could be explained on the bases of FTIR spectra of P(AAm-MA)-K-NR and P(AAm-MA)-M-NR given in Figure 4. C=O groups connected to the amide groups give absorption peak at 1676 and 1681 cm^{-1} for P(AAm-MA)-K-NR and P(AAm-MA)-M-NR, respectively. The weak peak at 1559 cm^{-1} is because of olefinic C=C stretching band of dye in P(AAm-MA)-K-NR and P(AAm-MA)-M-NR. Aliphatic C—N stretching band is observed at 1100–1150 cm^{-1} in all structure, while aromatic C—N band is observed at 1380–1400 cm^{-1} in P(AAm-MA)-K-NR and P(AAm-MA)-M-NR. A possible interaction between the polymeric composites and dye molecules is shown in Scheme 1. The interaction between the cationic groups on the dye and carboxyl groups of adsorbents is ion–ion interaction. These may occur between the negative charge of carboxyl groups on the adsorbent and the positive charge on the tertiary nitrogen atoms of the dye. Also, hydrophobic and hydrogen bonds may be takes place.

XRD analysis

The XRD patterns of the prepared adsorbent, Figure 5 reflect the interaction between the polymeric part and clay. The XRD pattern of kaolinite contains a reflection at $2\theta = 12.33°$, which indicates a basal spacing of 7.19 Å.[8] In case of P(AAm-MA)-K, the reflection at $2\theta = 12.55°$, indicating a basal spacing of 7.10 Å. It is clear that, there is no obvious difference of the typical diffraction peak and basal spacing between kaolinite and the corresponding P(AAm-MA)-K composite. This finding indicates that the reaction between PAAm and MA with kaolinite occurred on the surface without intercalating into the stacked silicate galleries. This could be attributed to that PAAm polymer chains cannot be

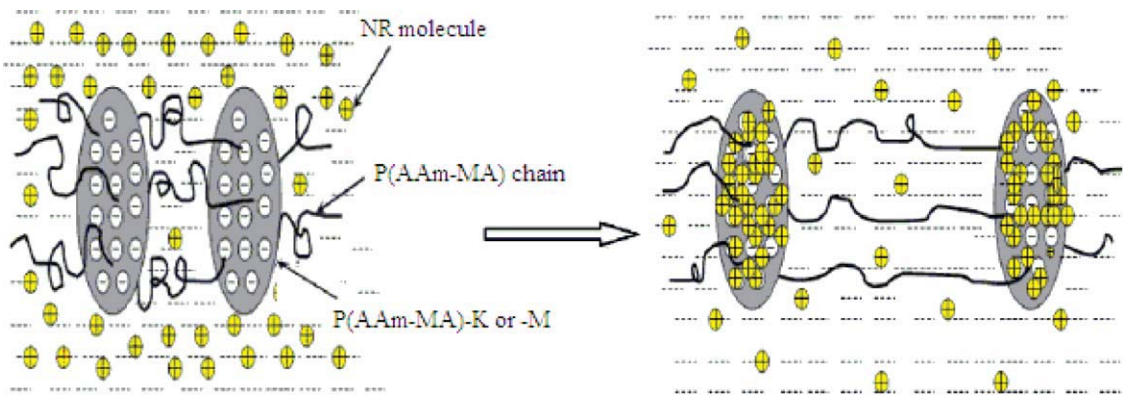

Scheme 1 Mechanism of NR adsorption onto P(AAm-MA)-K and P(AAm-MA)-M. [Color figure can be viewed in the online issue, which is available at www.onlinelibrary.wiley.com]

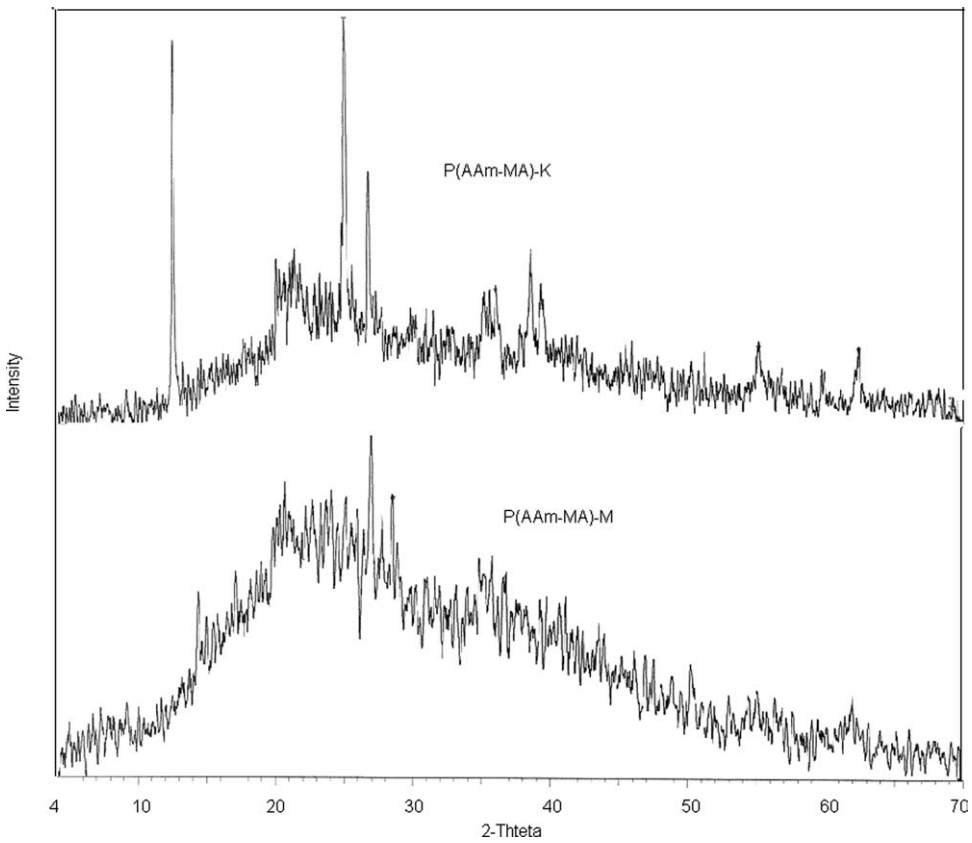

Figure 5 XRD patterns of P(AAm-MA)-K and P(AAm-MA)-M.

intercalated into the galleries of kaolinite, owing to the absence of permanent negative charges on the silicate galleries and the intensive hydrogen bond effect between layers.

The diffraction pattern of montmorillonite contains the main peak at $2\theta \sim 6.9^\circ$, which was attributed to the formation of the interlayer spaces by regular stacking of the silicate layers along the[001] direction. The interlayer distance estimated from this peak is 12.74 Å.[8] After incorporation of montmorillonite into PAAm polymeric network, the typical diffraction peak of montmorillonite disappeared (Fig. 5). This observation indicates the intercalation of polymeric network within montmorillonite and the exfoliation of montmorillonite as well.

SEM analysis

The dispersion of clay into polymer matrix was explained on the bases SEM imaging of the

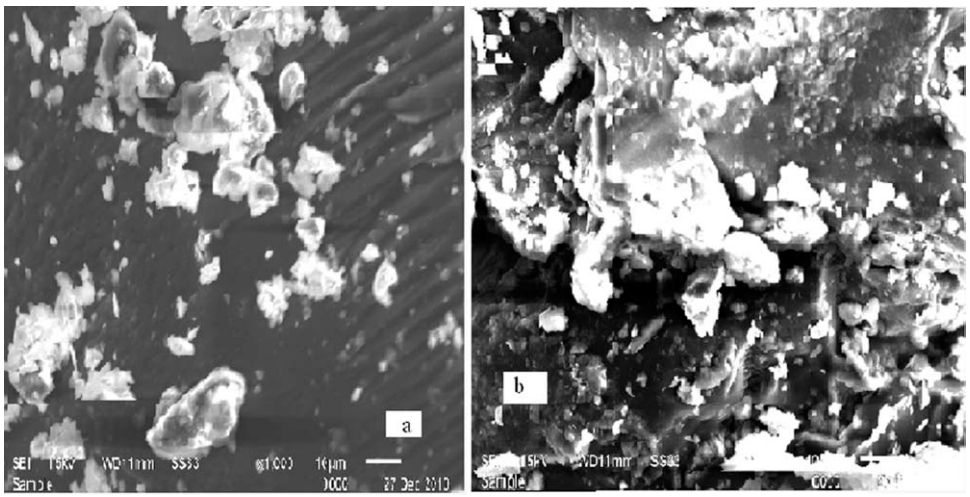

Figure 6 The scanning electron micrographs of P(AAm-MA)-K (a) and P(AAm-MA)-M (b).

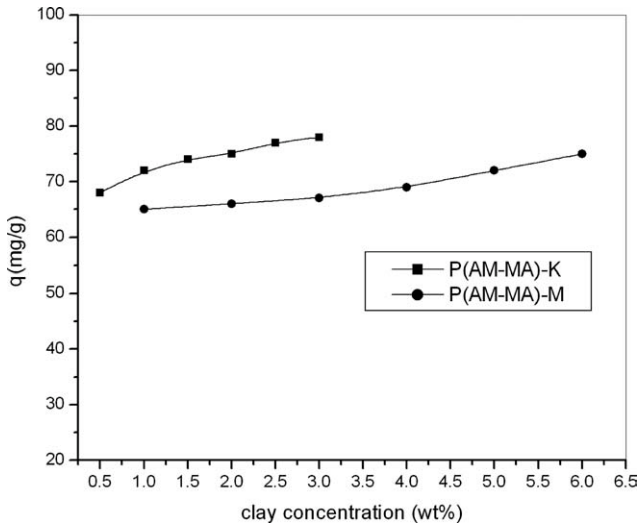

Figure 7 Effect of montmorillonite and kaolinite ratio present in P(AAm-MA)-K and P(AAm-MA)-M on its sorption capacity toward neutral red dye.

polymer/clay composites (Fig. 6). The micrograph clarify that the clay was substantially exfoliated and homogeneously dispersed throughout the polymer matrix. Therefore it could be concluded that fine and homogeneous clay dispersion are achieved in the polymer state. Also the rough surface structure with many pores may reflect the high capacity of the produced polymer/clay composites.

Effect of clay content in the composite

Figure 7 shows the variation in adsorbed amount of dye on P(AAm-MA)-K and P(AAm-MA)-M against clay content in the respective adsorbent. The interaction between the polymer and clay is not clearly identified. It could be generally regarded as being a combination of hydrogen bonding and ionic interaction.[20,21] Where the oxygen atoms on the clay surface may form hydrogen bonds with the amide proton of the polymeric moiety, and the metal ions on the clay surface may form a complex with the carboxyl groups on the polymeric moiety as mentioned above.

The amount of dye adsorbed was slightly increased with increasing the clay content in the composites. This finding could be explained as: increasing the clay concentration leads to an increase in the sorption sites and exchangeable cations (Na^+, Ca^{2+}) on the sorbent. Consequently, the incorporation of clay increased the number of ionizable groups in the polymer matrix. The neutral red dye when dissolved within these pH conditions forms cationic organic cations,[33] which could be exchanged with exchangeable cations on clay surface. Also, hydrogen bonding interaction takes place between the reactive —OH on the clay surface and -NR dye.

Effect of adsorbent amount

Adsorbent dose is an important parameter in the determination of adsorption capacity. The effect of adsorbent dose was investigated by stirring various amounts of composites with 20 mL of 100 mg L^{-1} NR aqueous solution at 25°C ± 1°C for 2 h. The results are shown in Figure 8(a,b). It was observed that the removal efficiency of P(AAm-MA)-K and P(AAm-MA)-M increased with increasing adsorbent dose from 1.5 to 7.5 mg L^{-1}. This observation could be explained as increasing adsorbent amount increases the specific surface area and availability of more adsorption sites. However, further increase in adsorbent amount did not give significant increase in removal efficiency. The adsorption capacity decreases as the adsorbent dose increases from 1.5 to 7.5 mg L^{-1}. The adsorbent dose was maintained at 0.01 g L^{-1} in all the subsequent experiments.

Effect of solution pH on dye uptake

pH plays an important role for the adsorption of dyes on the prepared polymers. The adsorption capacity of cationic dye on to composite polymers strongly

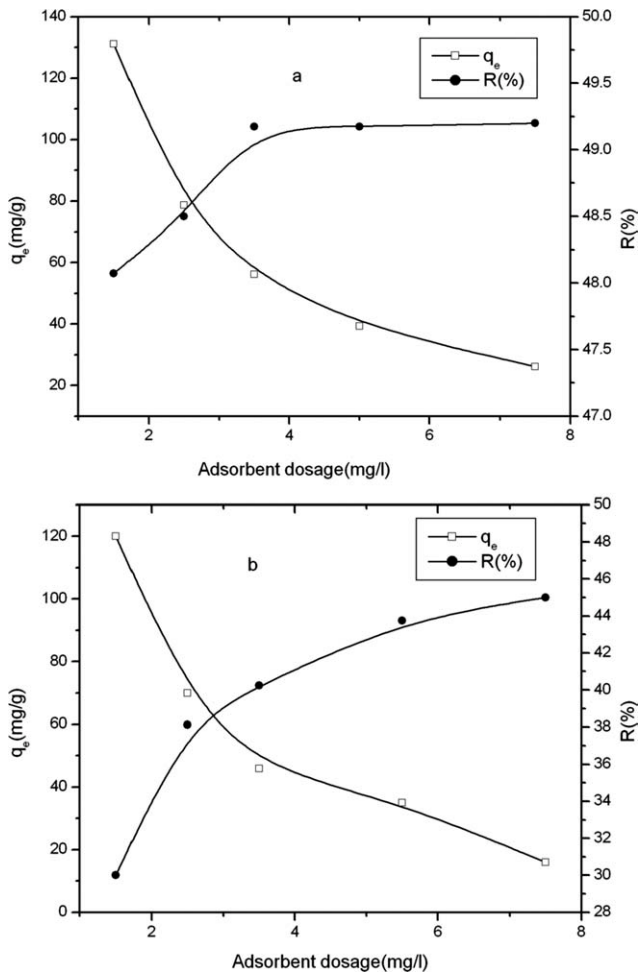

Figure 8 Effect of adsorbent dose on adsorption of NR onto P(AAm-MA)-K (a) and P(AAm-MA)-M (b) at 25°C.

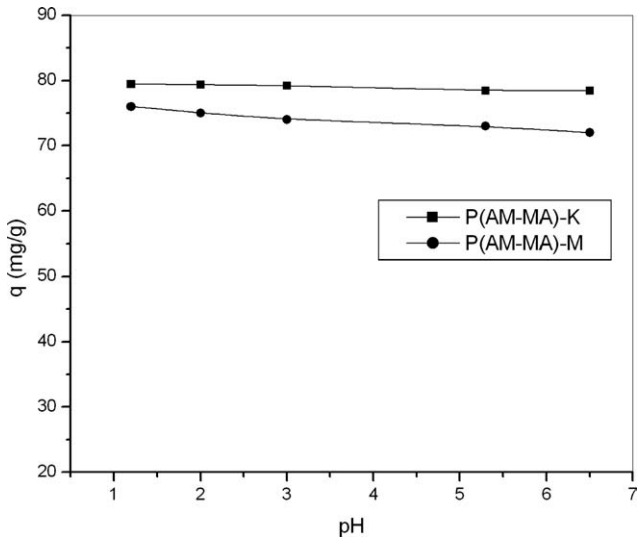

Figure 9 Effect of pH on the adsorption capacity of neutral red dye onto P(AAm-MA)-K and P(AAm-MA)-M at 25°C.

depends on surface charge, which eventually depends on the pH of the system. Zeta (ξ)-potential analysis indicated that the prepared polymeric composites P(AAm-MA)-K and P(AAm-MA)-M in potassium chloride solution were positively charged and have a ξ-potential of about 52 and 50 mV, respectively, at pH 5. The adsorption of NR dye upon P(AAm-MA)-K and P(AAm-MA)-M was studied from aqueous solutions of different pH within range 1–7. The results in Figure 9 clarify that the pH of dye solution slightly affects the adsorption reaction.

When dissolved the dye are positively charged ions[34] and will undergo attraction toward the anionic surface sites of the composite structure. PAAm is nonionic polymer,[35] and ionizable groups on the polymer were increased by the addition of maleic acid to acrylamide monomer. Therefore these resins have many carboxyl groups that can increase the interaction between the cationic groups of cationic dyes and carboxyl groups of resins. Other types of interactions between resins and dye may take part as hydrogen bonding and hydrophobic effects. Hydrophobic effects are specifically aqueous solution interactions. In the present case, it could involve the aromatic rings, methyl, and methene groups on the dyes molecules and the methene groups on the resins. Hydrogen bond could occur between amine group's nitrogen atom on the dye molecules and the carbonyl groups on resins.[36] Also electrostatic interactions between dye molecules and the resins must be taken in consideration. The possible mechanism for adsorption of NR dye onto P(AAm-MA)-K or P(AAm-MA)-M could be suggested as in the Scheme 1.

Effect of contact time

The contact time necessary to reach equilibrium depends on the initial dye concentration. It has been shown that the adsorption capacity increases with dye concentration. The effect of contact time on the adsorption of neutral red onto P(AAm-MA)-K and P(AAm-MA)-M at different initial neutral red concentrations at 25°C are illustrated in Figure 10(a,b), respectively. Firstly the adsorption of dye increased quickly with time till 90 min. A subsequent steady stage, with no significant increase in adsorption with time was observed. This finding could be explained as firstly, the adsorption occurs at polymer surface, so, a fast adsorption rate was observed. While a slow adsorption at the inner surface was observed because of pore diffusion of dye into polymer matrix. On the other hand, the system did not show any desorption of dye after long time of stirring.

Adsorption isotherms

Adsorption capacity of an adsorbent is rather dependant on the concentration of the adsorbed molecule

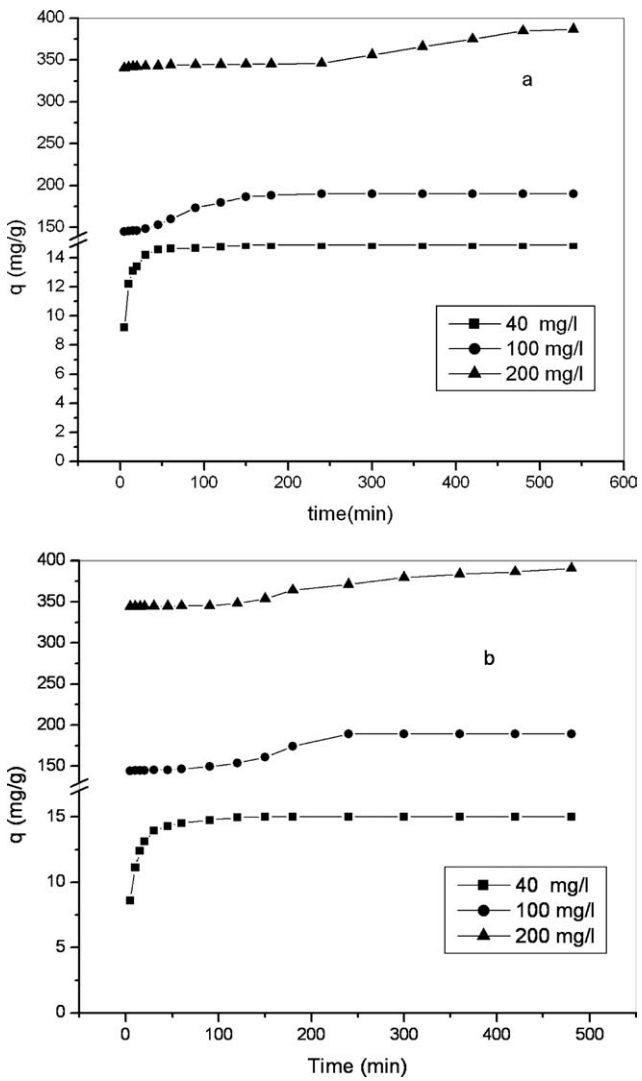

Figure 10 Effect of contact time on the adsorption of neutral red dye onto P(AAm-MA)-K(a) and P(AAm-MA)-M (b) at different initial dye concentrations at 25°C.

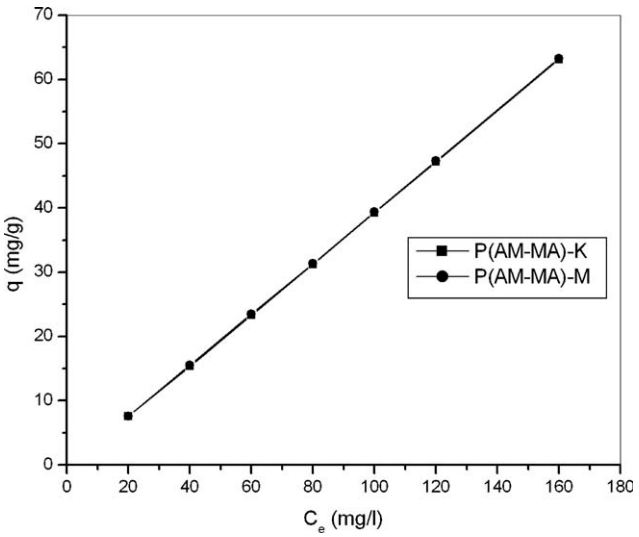

Figure 11 Equilibrium adsorption of neutral red onto P(AAm-MA)-K and P(AAm-MA)-M.

and other process parameters as well. The effect of initial dye concentration on adsorption capacity of resin was studied within the concentration range of (20–160 mg L^{-1}) at 25°C for 2 h. The results in Figure 11 show that as the initial dye concentration increased from 20 to 160 mg L^{-1} and the amount of dye adsorbed increased from 8 to 63 mg g^{-1}. Adsorption isotherms are important for the description of how molecules of adsorbate interact with adsorbent surface. A basic assumption of the Langmuir theory is that sorption takes place at specific homogeneous sites within the adsorbent.[37]Compared to the Langmuir isotherm, the Freundlich model is generally found to be better suited for characterizing multilayer adsorption process.[38] Langmuir isotherm model is represented by the following equation:

$$\frac{C_e}{q_e} = \frac{1}{bq_{\max}} + \frac{C_e}{q_{\max}} \tag{3}$$

where q_e (mg g^{-1}) is the amount adsorbed of dye molecules per unit weight of adsorbent at equilibrium concentration of the dye molecules in solution (C_e, mg L^{-1}). The $q_{\max}$ signifies the maximum adsorption capacity (mg g^{-1}) and b is a constant related to the energy of adsorption (L mg^{-1}). The essential characteristic of Langmuir equation can be expressed in terms of the dimensionless separation factor R_L, which is defined as:

$$R_L = \frac{1}{1 + b_{C_o}} \tag{4}$$

where C_0 is the initial dye concentration (mg L^{-1}) and b is the Langmuir constant. The value of R_L indicates the type of the isotherm either to be unfavorable ($R_L > 1$), linear ($R_L = 1$), favorable ($0 < R_L < 1$) or irreversible ($R_L = 0$).

Freundlich isotherm model is represented by the following equation:

$$\log_{q_e} = \log K_F + \frac{1}{n}\log C_e \tag{5}$$

where K_F and n are Freundlich constants that are related to adsorption capacity and intensity of adsorption, respectively.

Langmuir and Freundlich constants are calculated and given in Table II. The correlation coefficient values (R^2) of Langmuir isotherm are 0.990 and 0.999 for P(AAm-MA)-K and P(AAm-MA)-M, respectively. The adsorption capacities of both adsorbents were found to be comparable with those of other types of adsorbents (Table III). The calculated adsorption capacities were found to be close to the experimental results. The low value of R_L indicates a favorable adsorption reaction. The experimental data did not fit well with Freundlich isotherm model, where correlation coefficient values are 0.857 and 0.9388 for P(AAm-MA)-K and P(AAm-MA)-M, respectively. Generally, the experimental data were found to fit well with Langmuir isotherm model for both sorbents.

Sorption kinetics

The sorption kinetics was studied through a set of sorption experiments at constant temperature and monitoring the amount of dye adsorbed with time. The sorption process includes two stages; firstly a rapid removal stage followed by a much slower stage before reaching equilibrium. The sorption process could be controlled by different mechanisms including chemical reaction, diffusion control, and mass transfer. The kinetic parameters could help in

TABLE II
Langmuir and Freundlich Constants for the Adsorption of Neutral Red onto P(AAm-MA)-K and P(AAm-MA)-M

	Freundlich constants			Langmuir constants			
Sorbent	K_F (mg g^{-1})	n	R^2	$q_{\max}$ (mg g^{-1})	b (L g^{-1})	R_L	R^2
P(AAm-MA)-K	0.25×10^2	9×10^2	0.8570	380	5.5×10^2	0.1	0.990
P(AAm-MA)-M	1.01×10^3	0.33	0.9388	398	4.07×10^3	2.3×10^{-4}	0.999

TABLE III
Adsorption Capacities of Neutral Red Dye on Some Adsorbents Cited in the Literature

Adsorbent	q_{max} (mg/g)	Reference
P(AAm-MA)-K	380	Present study
P(AAm-MA)-K	398	Present study
Natural clay	567	39
Modified rice straw	188.68	40
Granular kohlrabi peel	122.36	41
Peanut hull	87.72	42
Halloysite nanotubes clay mineral	54.85	43
Mn-impregnated activated carbons	217.39	44

prediction of adsorption rate, adsorption mechanism, and give important information for designing and modeling the adsorption processes. The experimental adsorption data of neutral red dye onto P(AAm-MA)-K and P(AAm-MA)-M were analyzed using pseudofirst-order[44] and pseudosecond-order kinetic models.[45]

Assuming pseudo first-order-kinetics, the sorption rate could be evaluated using the simple Lagergren model, the earliest known model describing the adsorption rate based on the adsorption capacity. The differential equation of Lagergren model is expressed as follows:

$$\frac{dq_e}{dt} = k_1(q_e - q_t) \tag{6}$$

where q_e and q_t refer to the amount adsorbed (mg g^{-1}) at equilibrium and at time (t, min), respectively, and k_1 is the rate constant of pseudofirst-order adsorption (L min^{-1}). Integrating eq. (6) for the boundary conditions (from $t = 0$ and $q_t = 0$ to t and q_t) gives the equation

$$\log\left(\frac{q_e}{q_e - q_t}\right) = \frac{k_1}{2.303}t \tag{7}$$

which is the integrated rate law for a pseudofirst-order reaction. eq. (7) can be linearized as:

$$\log(q_e - q_t) = \log q_e - \frac{k_1}{2.303}t \tag{8}$$

Rate constant (k_1) and thetheoretical maximum adsorbed amount of (q_e) can be determined from the slope and intercept of the straight-line plots of log(q_e − q_t) against t, as represented in Figure 12. The plots show straight lines with good linearity, the values of the first order rat constant k_1, and the correlation coefficient (R^2) obtained from these plots are listed in Table IV. The slight difference in sorption kinetics between the two sorbents could be attributed to the structural difference existing between them. The first order mechanism suffered from inadequacies when applied for the sorption of neutral red dye onto P(AAm-MA)-K and P(AAm-MA)-M. One of the major discrepancies was observed when q_e values obtained from Lagergern plots were compared with the experimental q_e values Table IV. The experimental q_e values are different from the corresponding theoretical values for both the two sorbents. Thus good linearity of Lagergern plots is not a guarantee that the interaction of neutral red with the two sorbents P(AAm-MA)-K and P(AAm-MA)-M follow first order kinetics.

The conformity between experimental data and the model predicted values was expressed by the correlation coefficients (R^2, values close or equal to 1).

Second order kinetic model was applied upon the experimental data for prediction of sorption mechanism. The pseudo second order kinetic model is represented by the following differential equation:

$$\frac{dq_t}{dt} = k_2(q_e - q_t)^2 \tag{9}$$

where k_2 is the pseudosecond-order rate constant (g mg^{-1} min^{-1}). Integrating eq. (9) for the boundary conditions gives:

$$\frac{1}{(q_e - q_t)} = \frac{1}{q_e} + k_2 t \tag{10}$$

The above eq. (10) yields the linearized version of this model:

$$\frac{t}{q_t} = \frac{1}{k_2 q_e^2} + \left(\frac{1}{q_e}\right)t \tag{11}$$

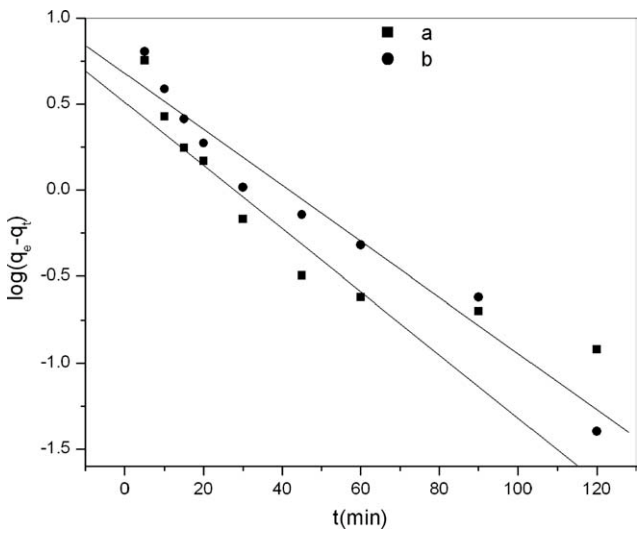

Figure 12 Adsorption kinetics of neutral red onto P(AAm-MA)-K (a) and P(AAm-MA)-M (b) according to pseudo-first-order model.

TABLE IV
Pseudo-First and Pseudo-Second Rate Constant for Neutral Red Dye onto Polymer

Sorbent	q_e(exp) (mg g^{-1})	Pseudo-first order kinetic			Pseudo-second-order kinetic			
		k_1 (L min^{-1})	q_e (cal) (mg g^{-1})	R^2	k_2 (g mg^{-1} min^{-1})	q_e(cal) (mg g^{-1})	h	R^2
P(AAm-MA)-K	15	5.5×10^{-3}	18	0.762	2.9×10^{-3}	15.2	0.66	0.999
P(AAm-MA)-M	15	5.8×10^{-4}	17	0.683	1.9×10^{-3}	15.3	0.44	0.999

The kinetic plots of t/q_t against t are shown in Figure 13. The linearity of the plots and the correlation coefficient (R^2) values suggest a strong relationship between the model parameters and explains that the sorption process could follow pseudo second order kinetics. The equilibrium sorption capacity (q_e), the initial sorption rate (h) ($h = k_2 q_e^2$, mg g min^{-1}), the pseudo second order rate constant (k_2) along with correlation coefficient (R^2) were determined and given in Table IV. Therefore the sorption reaction can be approximated more favorably by pseudo second order kinetic model and the over all rate constant of neutral red sorption onto P(AAm-MA)-K and P(AAm-MA)-M appears to be controlled by a chemisorptions process.

Desorption and regeneration

The economic feasibility of using adsorbent to remove contaminants from wastewater relies on its regeneration ability during multiple adsorptions/desorption cycles. In this study, various solutions were used for desorption of dye or regeneration of adsorbents in the batch system. The optimal desorption condition for dye was found to be 0.1*M* HCl, which showed desorption (up to 98.7%). Three adsorption desorption cycles were performed without significant decrease in adsorption capacity of adsorbents.

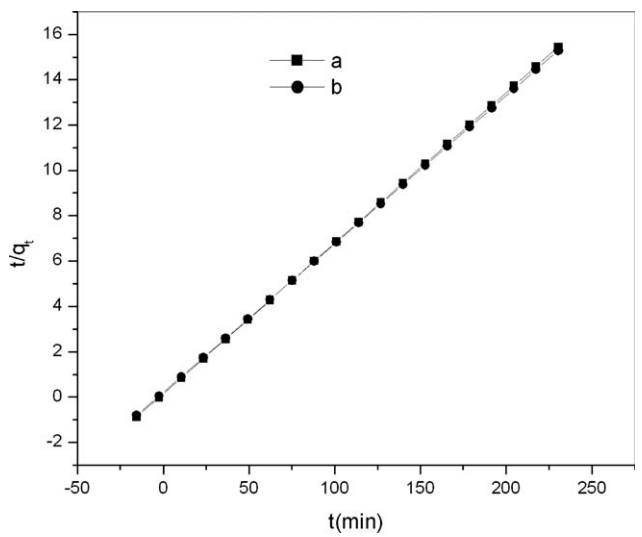

Figure 13 Adsorption kinetics of neutral red onto P(AAm-MA)-K (a) and P(AAm-MA)-M (b) according to pseudo-second-order model.

CONCLUSIONS

Poly(acrylamide-maleic acid)-kaolinite P(AAm-MA)-K and poly(acrylamide-maleic acid)-montmorillonite P(AAm-MA)-M were prepared by free radical aqueous polymerization, using *N*,*N*-Methylenebisacrylamide (NMBA) as a crosslinker and gamma rays as an initiator.

The batch sorption study revealed that P(AAm-MA)-K and P(AAm-MA)-M adsorbents could be employed as a potential adsorbent for the removal of neutral red dye from aqueous solutions. The maximum dye sorption capacity was found to be 398.4 and 396.8 mg L^{-1} at 25°C for P(AAm-MA)-K and P(AAm-MA)-M, respectively. The adsorption results were fitted with Langmuir isotherm model and could follow pseudosecond order kinetics. The R_L values showed favorable adsorption of dye onto P(AAm-MA)-K and P(AAm-MA)-M.

When compared with other adsorbents, P(AAm-MA)-K and P(AAm-MA)-M can be successfully used for the adsorption of neutral red dye from aqueous solutions.

References

1. Wang, J.; Liu, Z.; Guo, C.; Chen, Y.; Wang, D. Rapid Commun 2001, 22, 1422.
2. Ranade, A.; D'Souza, N. A.; Gnade, B.; Dharia, A. J Plast Film Sheeting 2003, 19, 271.
3. Mitzi, D. B. Chem Mater 2001, 13, 3283.
4. Novak, B. M. Adv Mater 1993, 5, 422.
5. Judeinstein, P.; Sanchez, C. J Mater Chem 1996, 5, 511.
6. Gilman, J. W.; Jackson, C. L.; Morgan, A. B.; Manias, E.; Giannelis, E. P.; Wuthenow, M.; Hilton, W.; Phillips, S. H. Chem Mater 2000, 12, 1866.
7. Wu, J. H.; Wei, Y. L.; Lin, S. B. Polymer 2003, 44, 6513.
8. Zhang, J.; Wang, A. React Funct Polym 2007, 67, 737.
9. Lee, W. F.; Yang, L. G. J Appl Polym Sci 2004, 92, 3422.
10. Kabiri, K.; Zohuriaan-Mehr, M. J. Macromol Mater Eng 2004, 289, 653.
11. El-Zahhar, A. A.; Abdel-Aziz, H. M.; Siyam, T. J Macromol Sci Part A Pure Appl Chem 2007, 44, 215.
12. Li, A.Wang, A. Q.; Chen, J. M. J Appl Polym Sci 2004, 92, 1596.
13. Lin, J.; Wu, J.; Yang, Z.; Pu, M. Macromol Rapid Commun 2001, 22, 422.
14. Wu, J.; Lin, J.; Zhou, M.; Wei, C. Macromol Rapid Commun 2000, 21, 1032.
15. Gao, D.; Heimann, R. B.; Lerchner, J.; Seidel, J.; Wolf, G. J Mater Sci 2001, 36, 4567.
16. Kampeerapappun, P.; Aht-ong, D.; Pentrakoon, D.; Srikulkit, K. Carbohydr Polym 2007, 67, 155.
17. Liu, P.; Zhang, L. Sep Purif Technol 2007, 58, 32.

18. Ghosh, D.; Bhattacharyya, K. G. Appl Clay Sci 2002, 20, 295.
19. Li, Y.; Zhang, B.; Pan, X. Compos Sci Technol 2008, 68, 1954.
20. Benco, L.; Tunega, D.; Hafner, J.; Lischka, H. J Phys Chem B 2001, 105, 10812.
21. McKay, G.; Otterburn, M. S. Water Air Soil Pollut 1985, 24, 307.
22. Yeh, R. Y. L.; Thomas, A. J Chem Tech Biotechnol 1995, 63, 55.
23. Kozuka, H.; Takagishi, T.; Yoshikawa, K.; Kuroki, N.; Mitsuishi, M. J Polym Sci A Polym Chem Ed 1986, 24, 2695.
24. Gao, B.; Wang, Y.; Yue, Q.; Wei, J.; Li, Q. Sep Purif Technol 2007, 54, 157.
25. Zhu, H.; Jiang, R.; Xiao, L. Appl Clay Science 2010, 48, 522.
26. Wang, Y.; Zeng, L.; Ren, X.; Song, H.; Wang, A. J Environ Sci 2010, 22, 7.
27. Ray, S. S.; Okamoto, M. Prog Polym Sci 2003, 28, 1539.
28. Alexandre, M.; Dubois, P. Mater Sci Eng 2000, 28, 1.
29. Juang, R.; Lin, S.; Huang, F.; Cheng, C. J Colloid Interface Sci 2004, 274, 337.
30. Liu, P. Appl Clay Sci 2007, 38, 64.
31. Theng, B. K. G. Formation and Properties of Polymer-Clay Complexes; Elsevier: New York, 1979.
32. Tyagi, B.; Chudasama, C. D.; Jasra, R. V. Spectrochimica Acta Part A 2006, 64, 273.
33. Gong, R.; Zhang, X.; Liu, H.; Sun, Y.; Liu, B. Bioresour Technol 2007, 98, 1319.
34. Runping, H.; Pan, H.; Zhaohui1, C; Zhenhui, Z; Mingsheng, T. J Environ Sci 2008, 20, 1035.
35. Farrokhpay, S.; Morris, G. E.; Fornasiero, D.; Self, P. J Colloid Interface Sci 2004, 274, 33.
36. Karada, E.; Saraydin, D.; Güven, O. Water Air Soil Pollut 1998, 106, 369.
37. Özcan, A; Özcan, A. S. J Hazard Mater 2005, B125, 252.
38. Crini, G.; Peindy, H. N. Dyes Pigm 2006, 70, 204.
39. Guiza, S.; Bagane, M.; Al-Soudani, A. H.; Ben Amore, H. Adsorpt Sci Technol 2004, 22, 245.
40. Gong, R.; Jin, Y.; Chen, J.; Hu, Y.; Sun, J. Dyes Pigm 2007, 73, 332.
41. Gong, R.; Li, M.; Yang, C.; Suna, Y.; Chenb, J. J Hazard Mater 2005, B121, 247.
42. Luo, P.; Zhao, Y.; Zhang, B.; Liu, J.; Yang, Y.; Liu, J. Water Res 2010, 44, 1489.
43. Zhang, J.; Shi, Q. Q.; Zhang, C. L.; Xu, J. T.; Zhai, B.; Zhang, B. Bioresour Technol 2008, 99, 8974.
44. Allen, S. J; Gan, Q.; Matthews, R.; Johnson, P. A. J Colloid Interface Sci 2005, 286, 101.
45. Ho, Y.S.; McKay, G. Process Biochem 1999, 34, 451.